

OPTICAL As Well As ARCHITECTURAL RESIDENCES OF Nb: TiO₂ SLIM MOVIES DEPOSITED BY DC MAGNETRON SPUTTERING AT AMBIENT TEMPERATURE

RAMAKRISHNA GODDETI, KEERTHANA D

Dept of H & S, Sree Dattha Group of Institutions, Hyderabad, Telangana, India

ABSTRACT:

This work reports on the influence of niobium on the structural and optical properties of titanium dioxide thin films made by DC Magnetron sputtering. The films were deposited on glass substrates at ambient temperature which stood at below 50 °C in the deposition chamber. Film thickness based on profilometry ranged from 432 nm to 620 nm. Parameters investigated among others include structure, optical constants, grain size and film density. The as-deposited films were found to be amorphous and turn to crystalline upon annealing in air. The film density increased with doping to a maximum estimated to be 5.77 at. % Nb, beyond which a decrease was recorded. It was also observed that the refractive index of the film increased with doping.

Keywords: *HPLC, PDA, stability indication method, drug.*

1. INTRODUCTION:

Titanium dioxide films are extensively used in optical thin film device applications owing to their appropriate optical properties, high thermal and chemical stability in hostile environments [1-8]. These films present good durability, a high transmittance in the visible spectral range, and a high refractive index. They are suitable for applications, such as antireflection coatings, multilayer optical coatings, optical waveguides, etc. Due to their unusually high dielectric constant, titanium dioxide thin films are attractive materials for fabricating capacitors. Impurity doping induces substantial modifications in electrical and optical properties of semiconductor materials [9,10]. Several methods can be used to deposit thin films [11,12]. One of the most utilized methods for obtaining uniform and dense titanium dioxide thin films as well

as for large area deposition, with well-controlled stoichiometry, is reactive sputtering. Thin film properties are very much sensitive to the deposition environment and as such several parameters that may influence film properties can be studied. In this work, the effect of niobium doping on optical, structural and electrical properties of titanium dioxide is investigated.

Thin films of niobium doped titanium dioxide were deposited on unheated and heated plain glass substrates (microscope slides) by reactive D.C. Magnetron sputtering in a deposition system based on a Balzers UTT 400 unit in an argon and oxygen atmosphere with gas flow rates set at 60.0 and 4.0 sccm respectively. Two targets were used - Nb target with purity 99.999% and Ti target with purity 99.99%. Doping by Nb was achieved by setting the target power

at 20 Watts, 40 watts, 60 watts and 80 watts while the Ti target power was fixed at 350 watts. The deposition time for all the films was 21 minutes. The working pressure was maintained at 13.26 mTorr. Before deposition, the chamber was pumped down to 1.4×10^{-6} mbar (1.05×10^{-3} mTorr) and baked for 8 hours. After deposition, the films were annealed in air at 500 °C for 30 minutes. Thickness measurement was carried out using Alpha Step Profilometer while Perkin Elmer λ 900 Spectrophotometer was used to measure reflectance and transmittance in the range 300 – 2550 nm. The interference fringe method developed by Swanepoel [15] was used to determine the optical constants and to confirm the film thickness. RBS and ERDA were used to determine film composition with films deposited on silicon substrates while crystal structure was determined using D5000 Xray Diffract meter.

2. RELATED STUDY:

Five samples of TiO₂ with varying niobium doping were characterized and subsequently analyzed (Table 1). Film composition deduced by RBS and ERDA for two films having different niobium content is shown in Fig. There is good agreement between RBS and ERDA data as demonstrated by the results of two samples containing 3.59 at. % Nb and 5.77 at. % Nb shown in Figs. respectively. For instance, ERDA estimation of Nb content in T4D film is about 5.6% while RBS gives 5.77%. Further analysis of RBS and ERDA data show niobium content increased almost linearly with target power as presented in Fig.

As revealed by the XRD pattern in Fig. 5, the as-deposited films were amorphous and this was true for all samples before annealing. Upon annealing in air, all samples adopted a crystalline structure as shown in Fig. 6. Undoped TiO₂ film showed a preferential orientation along the (004) plane at $2\theta = 37.8^\circ$. The inter-plane spacing (d) values were compared with the standard JCPDS data card (00-021-1272) which corresponds to the anatase phase. As niobium concentration increased in the film, the intensity of the peak corresponding to the plane (004) decreased and that of (101) increased.

3. PROPOSED METHODOLOGY:

The grain size of the films was estimated using the Debye-Scherrer formula, $D = (0.9\lambda)/(\beta \cos \theta)$, where D is the diameter of the crystallites forming the film, λ is the wavelength of CuK α line, β is FWHM in radians and θ is the Bragg angle. The grain size was found to remain almost constant then increase drastically at higher dopant level (8.5 at. %) as shown in Fig. 7. The XRD spectra for T4E show a systematic shift to low angles which we attribute to strain induced by the dopant atoms. When the XRD peak intensities for T4E and T4D are compared (Fig.), it is found that the former yields peaks of lower intensity indicating lower degree of crystallinity as compared to T4D.

where ρ_{areal} is the areal density in atoms/cm² obtained from the fit of RBS spectra using SIMNRA program, MW is the molecular weight of the elements in grams/mole, NA is Avogadro's number, and

tf is the thickness of the film in Å. The density is plotted in Fig. The film density increases with doping but at higher dopant concentration, it starts to decline. The decline could be attributed to the larger grain size which might reduce the packing fraction of the film.

All the films have a high transmittance in the measured range as shown in Fig. Upon annealing in air, the spectra shift to the shorter-wavelength region due to reduced thickness of the film. The transmittance is also slightly higher indicating reduced absorption especially in the wavelength below 1000 nm.

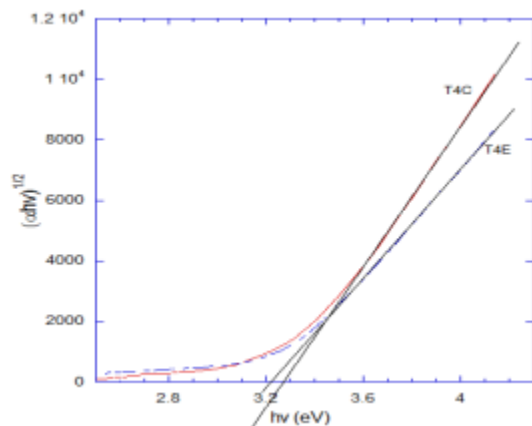


Fig.3.1. A plot of $(\alpha hv)^{1/2}$ against photon energy (hv) used to determine the band gap.

5. CONCLUSION:

This work has shown that films deposited under the conditions used produce films which are amorphous which turn to crystalline upon annealing in air. The refractive index of the films increases with the dopant concentration. It has also been

noted that the niobium doping increases almost linearly with power applied on its target. There was also a shift in bandgap to lower energies with doping

REFERENCES:

[1] R. B. Boom and H. A. Peterson, "Superconductive energy storage for power systems," IEEE Trans. Magn., vol. MAG-8, pp. 701–704, Sept. 1972.

[2] R. F. Giese, "Progress toward high temperature superconducting magnetic energy storage (SMES) systems—A second look," Argonne National Laboratory, 1998.

[3] , "Progress toward high temperature superconducting magnetic energy storage (SMES) systems—A second look," Argonne National Laboratory, 1998.

[4] C. A. Luongo, "Superconducting storage systems," IEEE Trans. Magn., vol. 32, pp. 2214–2223, July 1996.

[5] V. Karasik, K. Dixon, C. Weber, B. Batchelder, and P. Ribeiro, "SMES for power utility applications: A review of technical and cost considerations," IEEE Trans. Appl. Superconduct., vol. 9, pp. 541–546, June 1999.

[6] I. D. Hassan, R. M. Bucci, and K. T. Swe, "400 MW SMES power conditioning system development and simulation," Trans. Power Electron., vol. 8, pp. 237–249, July 1993.

[7] Q. Jiang and M. F. Conlon, "The power regulation of a PWM type superconducting magnetic energy storage unit," IEEE Trans. Energy Conversion, vol. 11, pp. 168–174, Mar. 1996.

[8] D. Lieurance, F. Kimball, C. Rix, and C. Luongo, "Design and cost studies for small

scale superconducting magnetic energy storage systems,” IEEE Trans. Appl. Superconduct., vol. 5, pp. 350–353, June 1995.

[9] J. McDowall, “Conventional battery technologies—Present and future,” in Proc. 2000 IEEE Power Engineering Society Summer Meeting, vol. 3, July 2000, pp. 1538–1540.

[10] M. A. Casacca, M. R. Capobianco, and Z. M. Salameh, “Lead-acid battery storage configurations for improved available capacity,” IEEE Trans. Energy Conversion, vol. 11, pp. 139–145, Mar. 1996.